Laser scanning cytometry and tissue microarray analysis of salinity effects on killifish chloride cells

Raquel N. Lima and Dietmar Kültz*

University of California, Davis, One Shields Avenue, Davis, CA 95616, USA

*Author for correspondence (e-mail: dkueltz@ucdavis.edu)

Summary

The effects of salinity on chloride cells (CC) and Na^+/K^+-ATPase content in gill epithelium of euryhaline killifish *Fundulus heteroclitus* were analyzed using laser scanning cytometry (LSC) and tissue microarrays (TMAs). Salinity acclimations consisted of acute transfer from freshwater (FW) to 1× seawater (SW) and gradual transfer from FW to 2.4× SW. Suspensions of dissociated gill epithelial cells were stained with DASPMI and evaluated using LSC. CC number and volume are proportional to external salinity, being lower in FW ($0.5\pm0.2\times10^5$ and 405 ± 32 μm^3, respectively) and higher after 5 weeks in 2.4× SW ($3.7\pm0.9\times10^5$ and 2697 ± 146 μm^3, respectively). TMAs were constructed from fixed gill tissues and developed using antibody for Na^+/K^+-ATPase to visualize CCs *in situ* and compare their characteristics with isolated CCs. Na^+/K^+-ATPase content per CC increases transiently (from $2.2\pm0.5\times10^6$ to $4.8\pm1.1\times10^6$ relative fluorescence units, RFU) after 1 week of acute acclimation to 1× SW but returns to baseline values ($2.4\pm0.5\times10^6$ RFU) within 5 weeks. In contrast, gradual acclimation to 2.4× SW permanently increases Na^+/K^+-ATPase content per CC (from $2.0\pm0.8\times10^6$ to $6.7\pm2.7\times10^6$ RFU after 5 weeks). CC size *in situ* did not correlate well to salinity because of basolateral membrane infoldings. Taken together, these data suggest that euryhaline fishes are capable of sensing environmental salinity to utilize transient short-term and permanent long-term adaptations for coping with salinity changes. These results also demonstrate the power of LSC and TMA for comparative biology.

Introduction

Chloride cells (CC) in gills of euryhaline teleosts are highly differentiated ion-transporting cells that are characterized by an enormous energy turnover, as indicated by the great abundance of mitochondria and ATPases (Karnaky, 1986). In response to changes in environmental salinity, important morphometric properties of CC and abundance of many membrane transport proteins are regulated to accommodate the altered requirements for transcellular ion transport across the gill epithelium and to maintain plasma ion homeostasis.

In this study we utilize laser scanning cytometry (LSC) and tissue microarrays (TMAs) for quantitative analysis of salinity effects on CC and Na^+/K^+-ATPase in gills of the euryhaline killifish *Fundulus heteroclitus*. We hypothesize that using this approach it is possible to compare salinity effects on chloride cell properties *in situ* and in dissociated gill cell suspensions and that this will enable us to better understand the kinetics of adaptation during acute and gradual salinity increase. A major advantage of the TMA-LSC approach is its high-throughput capability and extraordinary sensitivity in recording fluorescence-based properties of thousands of individual chloride cells in a very short time. In addition, because TMAs

array all samples of one or more experiments on a single slide they can be stained and analyzed under identical conditions. Thus, immunohistochemistry and other fluorescence-based measurements using this technique are highly quantitative when comparing salinity effects in different samples.

Laser scanning cytometry (LSC) was developed as a hybrid-technology merging the advantages of laser scanning fluorescence microscopy and flow cytometry (Kamentsky, 2001). Tissue microarrays (TMAs) are an ideal complementary technology to LSC because they permit high-throughput analysis of many tissue samples simultaneously under identical conditions, thus minimizing sample-to-sample variation. TMAs were originally developed to accelerate the scoring of tumor tissues for clinical pathology (Bubendorf et al., 2001). However, because of their versatility TMAs are increasingly popular for many other applications in biological research and they promise to become a powerful tool for comparative experimental biology. Using LSC and TMA technology it is possible to perform large-scale analyses of proteins, e.g. by immunophenotyping (Mocellin et al., 2001), of DNA, e.g. by nuclear DNA staining (Buse et al., 1999) and of RNA, e.g. by

fluorescence *in situ* polymerase chain reaction (Pachmann et al., 2001). Such LSC/TMA-based analyses are much faster, less error-prone and more cost-efficient than other approaches.

Using this novel approach we have investigated the kinetics of CC hypertrophy and proliferation as well as Na^+/K^+-ATPase abundance in CC of killifish gill epithelium after exposure of fish to acute and gradual salinity acclimation regimens.

Materials and methods
Animals and acclimation procedures

Killifish *Fundulus heteroclitus* L. were collected on Mount Desert Island, Maine, USA in a brackish water (estuarine) habitat. They were then transported to Davis, California, USA and acclimated for more than 1 month to freshwater (FW: Na^+=28 mg l^{-1}, K^+<5 mg l^{-1}, Ca^{2+}=33 mg l^{-1}, Mg^{2+}=36 mg l^{-1}, pH 8.0) in circular flow-through tanks of 1 m diameter. Fish were fed commercial trout pellets *ad libitum*. The water temperature was 18°C and the photoperiod was set to 12 h:12 h L:D during all experiments. Seawater (SW) used for experiments was prepared from synthetic sea salt (Red Sea Fish Farm, Israel) and the final salinity adjusted using a freezing point osmometer (Advanced Micro Osmometer, model 3300; Norwood, MA, USA). All salinity acclimation experiments were performed in 100 l closed circulation aquaria equipped with external power filters and aeration. Prior to acclimations fish were allowed to adjust to these aquaria in FW for 2 days. Hyperosmotic stress was induced by transferring fish from FW to SW according to the acclimation regimens illustrated in Fig. 1.

Gill perfusion, cell dissociation and live cell staining

At each sampling point during the acclimation experiments fish were killed by exposure to a lethal dose of MS-222
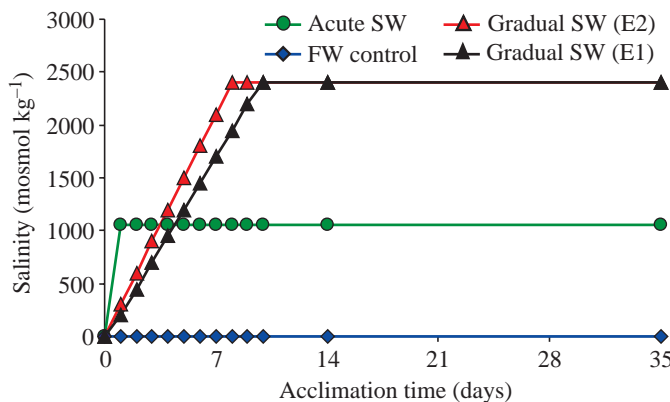

Fig. 1. Salinity acclimation regimens used in this study. Killifish were subjected to either acute transfer from freshwater (FW) to 1× seawater (SW, 1000 mosmol kg^{-1}, green circles) or to gradual transfer from FW to 2.4× SW (2400 mosmol kg^{-1}). During gradual transfers the salinity was increased either at a rate of 300 mosmol kg^{-1} per day (red triangles) or 250 mosmol kg^{-1} per day (black triangles) until it reached 2400 mosmol kg^{-1}. FW controls were transferred once on the first day to FW (blue diamonds).

(0.4% aminobenzoic acid-ethylether-methanesulfonate). The pericardium was opened and the gills perfused *via* the bulbus arteriosus with ice-cold phosphate-buffered saline (PBS: 146 mmol l^{-1} NaCl, 3 mmol l^{-1} KCl, 15 mmol l^{-1} NaH_2PO_4, 15 mmol l^{-1} Na_2HPO_4, 10 mmol l^{-1} $NaHCO_3$, pH 7.4; osmolality=330 mosmol kg^{-1}). After blood had been removed and gills had turned white (ca. 1–3 min) individual gill arches were dissected. All four gill arches of the left side were rinsed in PBS and fixed in 4% paraformaldehyde for immunohistochemistry (see below). All four gill arches of the right side were rinsed with PBS and the gill epithelium was scraped off the cartilage and cells dissociated as previously described (Kültz and Somero, 1995). Cell suspensions were stained with DASPMI (10 µmol l^{-1}) for 30 min and washed twice in PBS. After resuspension in 200–300 µl PBS an 80 µl sample was placed on a microscope slide and covered with a 60×24 mm coverslip. Preliminary experiments established that 80 µl are optimal for complete coverage of the entire area under the coverslip without any excess liquid remaining in the uncovered area of the slide. Slides were then evaluated using LSC (see below).

Tissue microarray construction and immunohistochemistry

Gill arches were fixed in 4% paraformaldehyde for at least 48 h and the fixative was changed once before embedding the tissue in paraffin (Tissue Prep 2, Fisher Scientific, Pittsburgh, PA, USA). These paraffin blocks were then used as donor blocks for tissue microarray (TMA) construction. An empty paraffin block served as a recipient block for TMA. TMA construction was done with a MTA-1 tissue microarrayer (Beecher Instruments, Sun Prairie, WI, USA) equipped with a set of 1 mm diameter punches as described previously (Kononen et al., 1998). Fixed and paraffin-embedded specimens of gill tissue from all acclimation groups were arrayed in the same recipient block and 4 µm sections of this block were taken using a microtome (Bromma 2218 Historange, LKB, Uppsala, Sweden) and floated onto poly-L-lysine coated slides. The slides containing the arrayed samples were dried overnight. When completely dry they were deparaffinized three times for 5 min each in xylene, twice for 5 min each in 100% ethanol, twice for 5 min each in 95% ethanol, and once for 5 min in 80% ethanol. After deparaffinization the slides were incubated for 30 min in blocking solution (PBS containing 1% bovine serum albumin) and for another 30 min in blocking solution containing 2% purified mouse IgG. Primary antibody against avian Na^+/K^+-ATPase α-subunit developed by Douglas M. Fambrough was obtained from the Developmental Studies Hybridoma Bank instituted under the auspices of National Institute for Child Health and Human Development (NICHD) and maintained by the University of Iowa, Department of Biological Sciences, Iowa City, IA 52242, USA. The antibody was diluted in blocking solution to a final concentration of 1% and the slides incubated in this solution at room temperature for 60 min. Slides were rinsed three times for 5 min each in PBS and incubated for 30 min with secondary goat anti-mouse IgG

antibody covalently bound to PacificBlue (P-10993, Molecular Probes, Eugene, OR, USA) at a final concentration of 0.5% in blocking solution at room temperature in the dark. Slides were rinsed again three times for 5 min each in PBS, topped with a coverslip, and sealed with nail polish. They were stored in the dark until analyzed by LSC.

Laser scanning cytometry

A Laser Scanning Cytometer (LSC, Compucyte, Cambridge, MA, USA) was used to analyze suspensions of dimethylaminostyrylmethylpyridiniumiodine (DASPMI)-stained gill cells and slides containing gill TMAs. For analysis of chloride cells (CC) in gill cell suspensions we used a 20× objective (UPlanFl 20×/0.50/∞/0.17, Olympus, Melville, NY, USA) in combination with the LSC argon laser (488 nm). For analysis of TMA slides processed by immunohistochemistry we used a 40× objective (UPlanFL 40×/0.75/∞/0.17, Olympus) in combination with the LSC UV laser (400 nm). Contouring and event segmentation variables were adjusted for optimal detection of CCs as identified by high DASPMI fluorescence in live cell suspensions and by Na^+/K^+-ATPase/Pacific Blue fluorescence in TMAs using WinCyte software (Compucyte). For each CC detected during scanning we recorded the area, fluorescence integral and maximum pixel fluorescence, among other variables using WinCyte software. Fluorescence intensities are expressed as relative fluorescence units (RFU). Wincyte software also automatically recorded the exact coordinates of each CC on the slide and the number of CCs in the scan area. These features enabled us to rapidly and reliably record the properties of thousands of CCs in isolated cell suspensions and of hundreds of CCs in TMA sections. In addition, the recorded coordinates for each CC made it possible to use the LSC relocation function to visually inspect particular subpopulations of CCs after each scan. For live CC analysis we used the same scan area of 8 mm×6 mm for each sample. For TMA analysis of fixed gill tissue we scanned an area with a diameter of 1 mm² for each sample. All data were stored automatically in electronic form in FCS file format.

Statistical analysis

CC numbers are expressed per fish and were calculated by multiplying the cells counted by the LSC with the scan area factor, the cell suspension volume factor and 2 (because only four of the eight gill arches were used for cell dissociation). The scan area factor equals 1400 μm² (effective slide area)/64 μm² (LSC scan area)=21.875. The cell suspension volume factor equals the volume that was used to resuspend the cells after DASPMI staining/80 μl (volume of cell suspension under the coverslip). Cell sizes are expressed as cell volume (μm³) for dissociated CC because they round up in suspension and volumes can be calculated based on the area measured with the LSC using the sphere formula. For CC *in situ*, cell sizes are expressed as the area measured in μm². All data are expressed as means ± standard error of the mean (S.E.M.) and the number of replicates is four animals for each salinity and time. Statistics software (KyPlot, http://www.kyenslab.com) was used to evaluate the significance of differences between treatment groups. The *F*-test was used to assess statistical differences of standard deviations. Depending on its result, either a paired *t*-test or the Mann–Whitney test was used to test for statistical significance between means of treatment groups. The significance threshold is $P<0.05$ for all tests.

Results

Rapid, reliable quantification of chloride cell properties by laser scanning cytometry

We have optimized a method using the LSC from Compucyte for quantitative analysis of CC properties in the euryhaline killifish (*F. heteroclitus*). This method is based on staining CC with the vital mitochondrial dye DASPMI (Bereiter-Hahn, 1976) and quantification of the fluorescence signal emitted by each CC after excitation by an argon laser at 488 nm. Dissociated CC from cell suspensions loaded onto microscope slides were segmented as individual events by the LSC software and contoured along their perimeter. For each of these events representing single CCs the fluorescence integral, maximum pixel, perimeter, *xy* coordinates on the slide, and area were recorded. When plotted as scattergrams with the ordinate representing CC area and the abscissa representing DASPMI maximum pixel fluorescence we could discern a region that contained a distinct cluster of events, which were confirmed to be CC by relocation and visual inspection of cells in this region using the LSC relocation function (Fig. 2A–C). Cells falling outside this region were not included in the analysis for the following reasons: (1) their fluorescence was too low and uncharacteristic of CC (events to the left of the region of analysis); (2) they were too small and represented fragments and debris generated during cell dissociation (events below the region of analysis); (3) they were too large and represented clusters of multiple cells rather than single cells (events above the region of analysis). After visual inspection of many events from a large number of samples taken from fish acclimated to various salinities we identified the minimum and maximum thresholds for CC area to be optimal when set at 30 μm² and 600 μm², respectively. Only cells having a maximum pixel DASPMI fluorescence of 12 000 RFU and higher were included in quantitative analysis because lower values were uncharacteristic for CC and indicative of other cell types containing fewer mitochondria that stain more weakly with DASPMI. Black circles in Fig. 2A–C identify CC whose area and DASPMI fluorescence correspond to mean values for each sample. Image galleries shown in Figs 4–6 were collected from those areas. When plotting the data as scattergrams with the ordinate representing CC area and the abscissa representing the integral CC fluorescence then CC within the region of analysis display a very strong linear relationship between these two parameters (Fig. 2D–F). This linear relationship is expected for CC because the density of mitochondria in CC is extremely high and their number is limited by the available space, which in turn depends directly on CC size. Thus, using
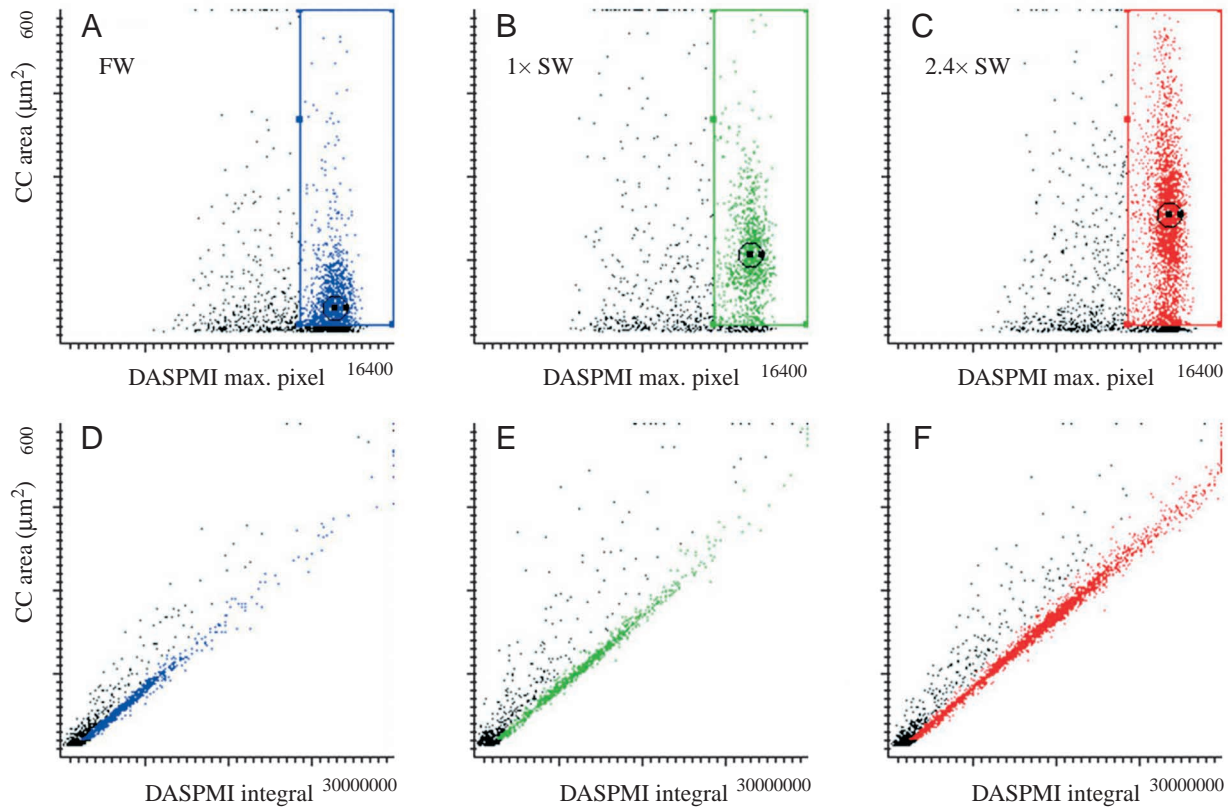
Fig. 2. (A–C) Laser scanning cytometry (LSC) analysis of chloride cells (CC) from killifish acclimated for 10 days to FW (blue), 1× SW (green) and 2.4× SW (red). CC were identified based on DASPMI fluorescence with the LSC. CC area and maximal intensity of DASPMI fluorescence were recorded for each CC during scanning by WinCyte software and plotted as scattergrams. (A) FW; (B) 1× SW; (C) 2.4× SW. The boxes enclose all accepted data and the circles enclose events that were used for generating image galleries with the LSC relocation function. (D–F) Additional scattergrams showing the relationship between CC area and integrated DASPMI fluorescence per CC were also recorded. (D) FW; (E) 1× SW; (F) 2.4× SW. CCs have higher DASPMI fluorescence than other cell types and are colored in all panels.
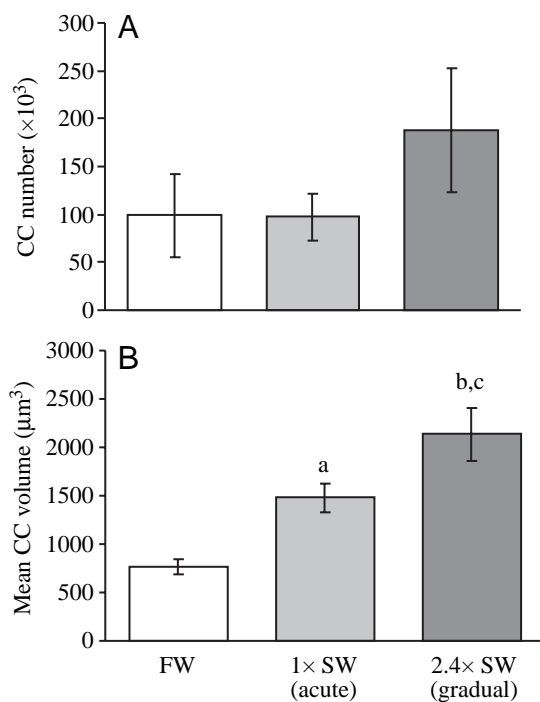
these optimized parameters for LSC analysis we were able to rapidly and reliably scan slides containing DASPMI-stained gill cell suspensions from many different fish.

Effect of intermediate term salinity acclimation on chloride cell properties

We acclimated killifish gradually to 2.4× SW by increasing the salinity by 250 mosmol kg^{-1} per day for a period of 10 days. Such intermediate term salinity acclimation was also done for two additional groups: acute transfer from FW to 1× SW and transfer from FW to FW, which served as a control. At the end of the 10 day acclimation period CC numbers and CC volumes from fish exposed to these different salinity acclimation regimens were evaluated by LSC analysis.

Fig. 3. Chloride cell (CC) number and size determined by LSC analysis from gill epithelial cell suspensions obtained after 10 days of acute and gradual acclimation from FW to SW. (A) CC number does not increase significantly after acclimation to 1× SW or 2.4× SW ($P>0.05$ in each case). (B) CC volume increases significantly after acclimation to 1× and 2.4× SW ($P<0.05$; [a]FW vs. 1× SW, [b]FW vs. 2.4× SW, [c]1× SW vs. 2.4× SW). $N=4$ animals for each salinity and time.
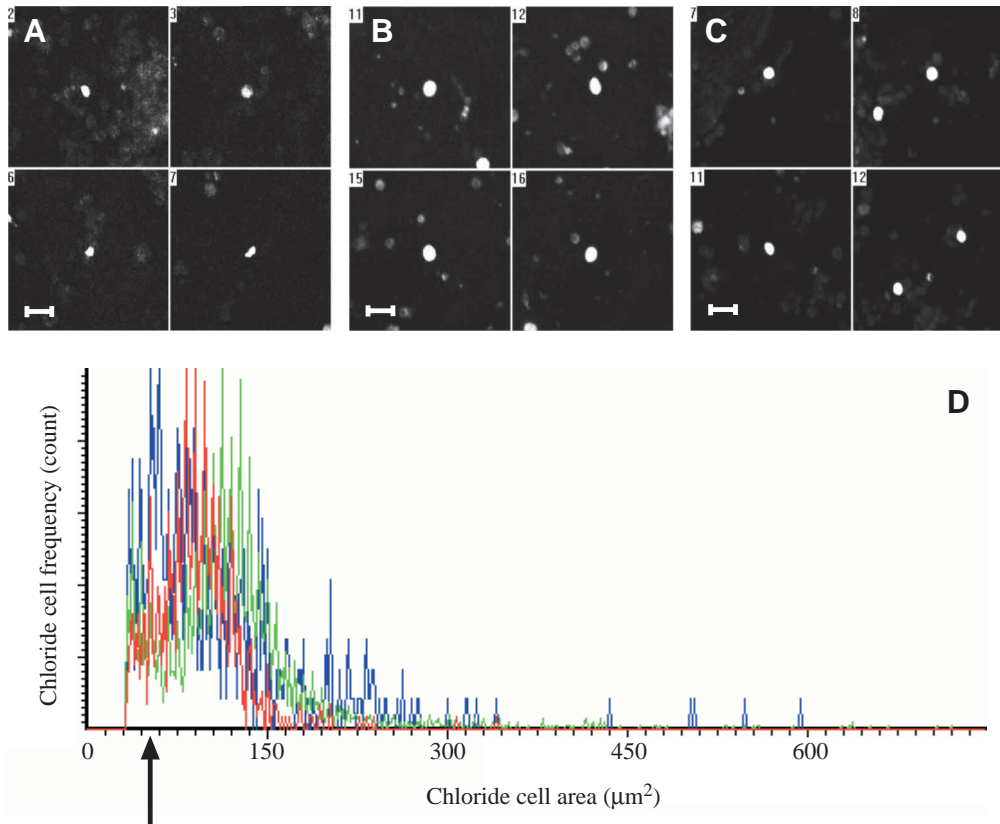
Fig. 4. Laser scanning images (A–C) and corresponding LSC histogram (D) of chloride cells (CC) from killifish exposed to FW, 1× SW or 2.4× SW for 1 week. Image galleries were acquired using the relocation function of the LSC. Cells shown in image galleries represent CC from within the circled areas in Fig. 2A–C. (A) CC from FW fish; (B) CC from 1× SW fish; (C) CC from 2.4× SW fish. (D) Histogram of CC area from fish acclimated to FW (blue), 1× SW (green) and 2.4× SW (red). The arrow points to a population of small cells that may represent accessory cells in the SW groups. Bars, 50 μm.

Interestingly, there is no significant increase in CC number after acute or gradual SW acclimation compared to FW controls, although a trend can be seen towards a higher number of CC in the group acclimated to the highest salinity of 2.4× SW (Fig. 3A). In contrast to CC number, the size of CC increases significantly after 10 days acclimation to SW, with the extent of the increase being proportional to the osmotic strength of the SW (Fig. 3B). The size of animals from the different groups was not significantly different and therefore not a factor that could explain the lack of a significant and salinity-dependent increase in CC numbers (data not shown). Therefore, killifish respond to intermediate term hyperosmotic stress by CC hypertrophy but not by an increase in CC number.

Effect of long-term salinity acclimation on chloride cell properties

Based on the data presented in Fig. 3 we carried out another series of experiments during which killifish were exposed to acute and gradual salinity acclimation for 5 weeks. During these experiments fish were sampled at 1, 2 and 5 weeks to assess intermediate- and long-term effects of acute and gradual salinity acclimation on CC number and size. Histograms depicting CC size distributions illustrate that salinity-induced CC hypertrophy was already apparent after 1 week (Fig. 4D) but continued to become more prominent after 2 weeks (Fig. 5D) and for the 2.4× SW group even more so after 5 weeks (Fig. 6D). Notably, besides a major peak for large CC in 1× and 2.4× SW acclimated fish a more minor peak was

consistently seen, falling within the same size range as the peak for FW CC (arrows in Figs 5D and 6D). Cells forming this peak were probably accessory cells. Image galleries depicting CC of mean size that corresponded to the peaks in the histograms in Figs 4D, 5D and 6D were acquired using the relocation feature of the LSC. Examples are shown in Figs 4A–C, 5A–C and 6A–C. Large CC size differences were particularly apparent after 5 weeks of acclimation (Fig. 6A–C). CC hypertrophy occurred rapidly in fish acutely exposed to 1× SW and the size of CC did not continue to increase significantly from 1 week to 5 weeks under these conditions (Fig. 7A). In contrast, CC hypertophy was absent after 1 week of gradual acclimation to 2.4× SW (the salinity at this time was 1200 mosmol kg⁻¹; see Fig. 1). Instead CC size in fish gradually acclimated to 2.4× SW reached that of fish acutely acclimated to 1× SW after 2 weeks and continued to increase dramatically at 5 weeks (Fig. 7A). Quantitative analysis of all samples revealed that CC numbers increased moderately by about twofold after 1–2 weeks of acute and gradual acclimation to 1× and 2.4× seawater (Fig. 7B). They continued to increase robustly and after 5 weeks CC numbers were fourfold higher in fish acclimated to 1× SW and sevenfold higher in fish acclimated to 2.4× SW compared to FW controls (Fig. 7B). CC hypertrophy displayed very different kinetics depending on the SW acclimation regimen. Differences in CC numbers and CC hypertrophy cannot be explained by fish size because total length of the animals did not differ significantly among experimental groups (data not shown).
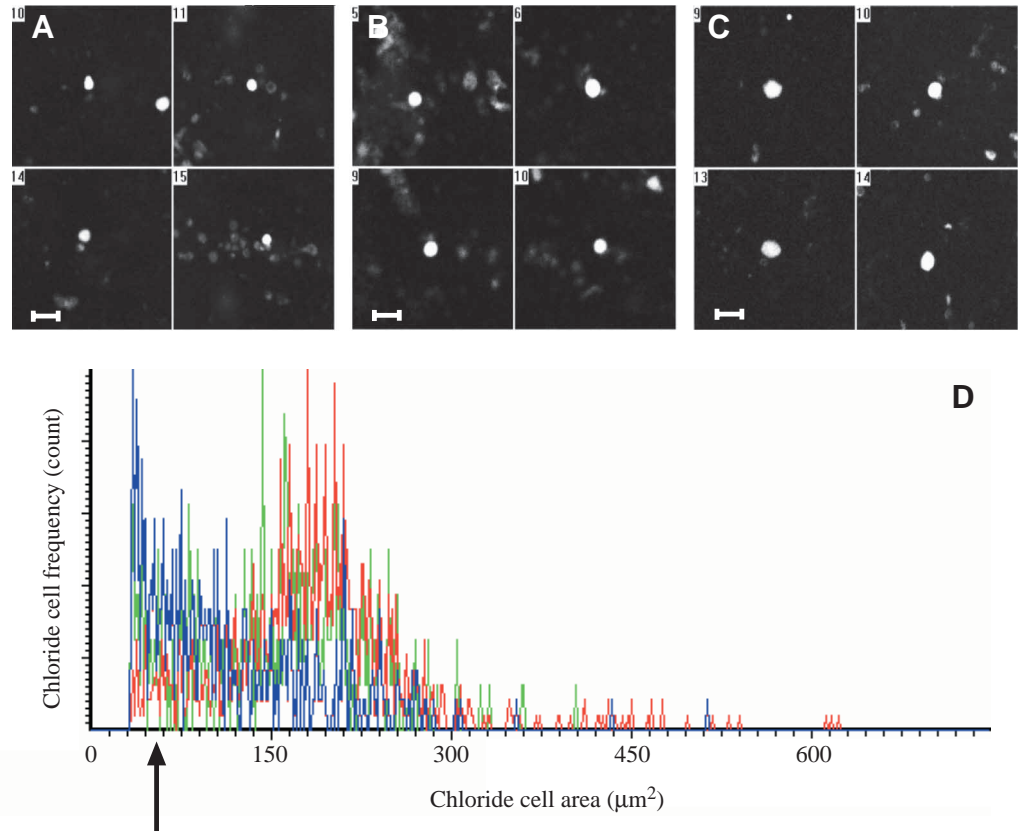
Fig. 5. Laser scanning images (A–C) and corresponding LSC histogram (D) of chloride cells (CC) from killifish exposed to FW, 1× SW or 2.4× SW for 2 weeks. Image galleries were acquired as described for Fig. 4. (A) CC from FW fish; (B) CC from 1× SW fish; (C) CC from 2.4× SW fish. (D) Histogram of CC area from fish acclimated to FW (blue), 1× SW (green) and 2.4× SW (red). The arrow points to a population of small cells that may represent accessory cells. Note the shift of CC to a larger area in the SW treatment groups compared to Fig. 4. Bars, 50 μm.
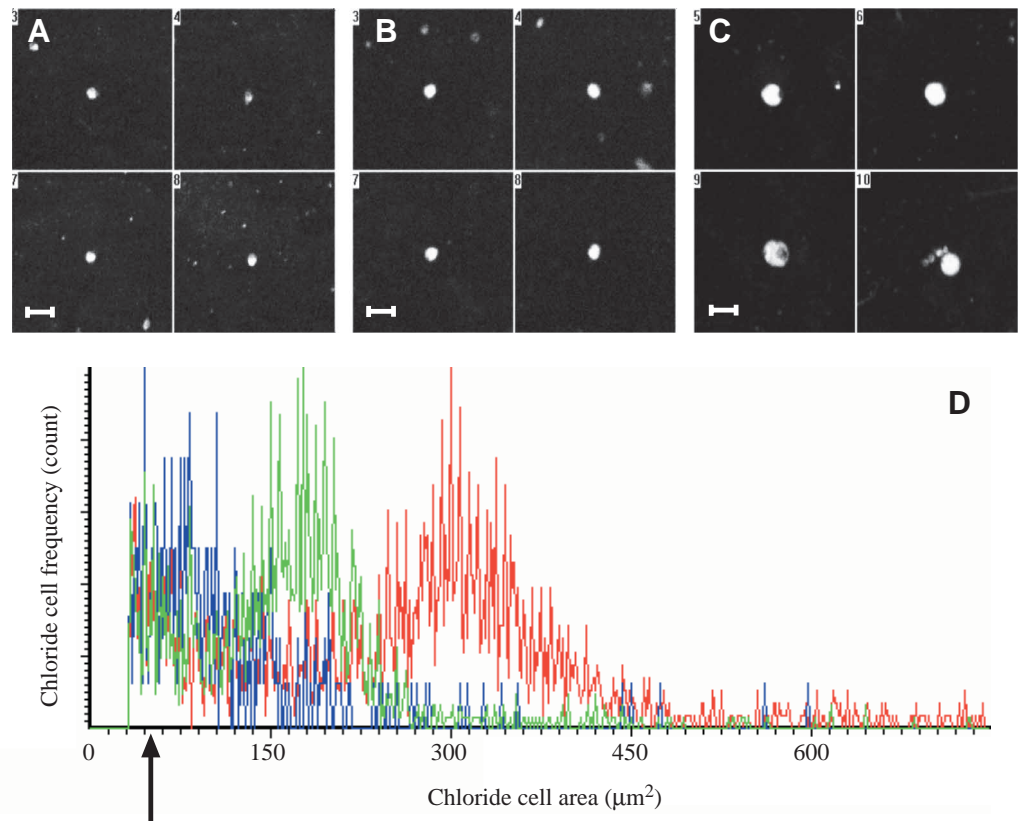

Fig. 6. Laser scanning images (A–C) and corresponding LSC histogram (D) of chloride cells (CC) from killifish exposed to FW, 1× SW or 2.4× SW for 5 weeks. Image galleries were acquired as described for Fig. 4. (A) CC from FW fish; (B) CC from 1× SW fish; (C) CC from 2.4× SW fish. (D) Histogram of CC area from fish acclimated to FW (blue), 1× SW (green) and 2.4× SW (red). The arrow points to a population of small cells that may represent accessory cells. Note the shift of CCs to a larger area in the 2.4× SW treatment group compared to Fig. 5. Bars, 50 μm.
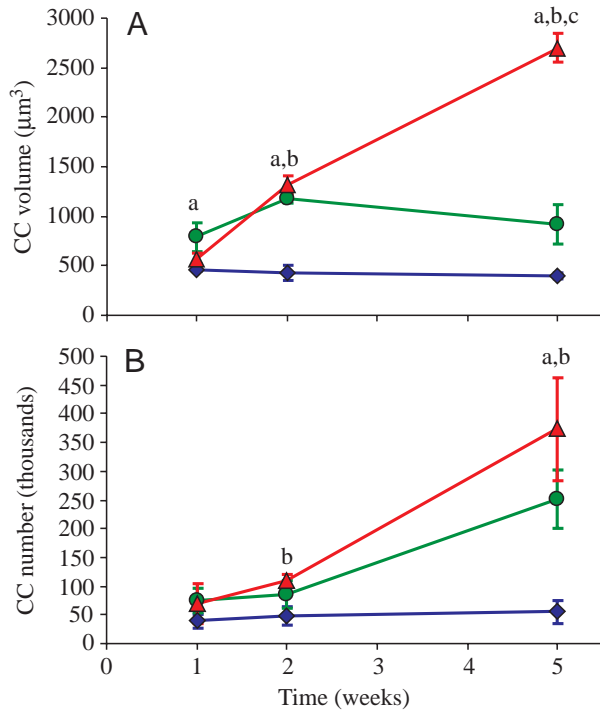
Fig. 7. Mean chloride cell (CC) number and size determined by LSC analysis from gill epithelial cell suspensions after acute or gradual acclimation from FW (blue diamonds) to 1× SW (green circles) or 2.4× SW (red triangles), respectively, *versus* acclimation period. (A) In the 1× SW group, CC volume is significantly larger at all the times analyzed ($P<0.05$) but does not continue to increase after 2 weeks. In contrast, during 5 weeks of 2.4× SW acclimation CC become significantly larger only after 2 weeks, but continue to increase ($P<0.05$). (B) CC number does not significantly increase until 2 weeks for 2.4× SW and until 5 weeks for 1× SW acclimation ($P<0.05$; [a]FW *vs*. 1× SW, [b]FW *vs*. 2.4× SW, [c]1× SW *vs*. 2.4× SW). $N=4$ animals for each salinity and time.

Tissue microarray analysis of chloride cells during salinity acclimation

Pieces of intact (non-dissociated) gill filaments from fish exposed to FW, 1× SW or 2.4× SW for 1, 2 and 5 weeks were arrayed on a microscope slide and stained with anti-Na$^+$/K$^+$-ATPase antibody and fluorescent secondary antibody as described in Materials and methods. An example of a Hematoxylin/Eosin-stained tissue microarray constructed from gill tissue is shown in Fig. 8A. By staining such arrays with a fluorescent antibody against Na$^+$/K$^+$-ATPase CC were identified as distinct and brightly fluorescent cells at the outer layer of gill filaments and at the base of the secondary lamellae (Fig. 8B). We have used the LSC for automatically contouring all fluorescent cells using the segmentation algorithm inherent in the LSC WinCyte software (Fig. 8C). For each sample on the slide the integral fluorescence per CC and the area of each CC were automatically measured during the LSC scan. The data for Na$^+$/K$^+$-ATPase abundance (= integral fluorescence) per CC are plotted in Fig. 8D. Similarly to the different kinetics of CC hypertrophy in fish exposed to 1× SW *versus* 2.4× SW

(see Fig. 7C) the kinetics of CC-specific Na$^+$/K$^+$-ATPase abundance also differs greatly in these two groups. While the Na$^+$/K$^+$-ATPase abundance per CC increases rapidly and transiently in fish transferred acutely to 1× SW, it increases more slowly but permanently in fish acclimated gradually to 2.4× SW (Fig. 8D). An advantage of LSC analysis is that the source of variation, which is particularly high for Na$^+$/K$^+$-ATPase abundance per CC after 5 weeks of gradual acclimation to 2.4× SW (±40.1%), can be traced to the level of individual animals because within each animal the cell-to-cell variation for Na$^+$/K$^+$-ATPase abundance in chloride cells is much lower for 2.4× SW at 5 weeks (±9.9, 9.8, 12.1 and 10.0%). This suggests that there are large individual differences in adaptability to very high salinities that approach the tolerance threshold for this species of euryhaline fish.

With regard to CC hypertrophy we observed the same trend in intact tissue specimens with the tissue microarray approach compared to evaluating dissociated suspensions of CC. The size of CC is smallest in FW fish and increases rapidly after acute transfer to 1× SW and more slowly but more steadily during gradual acclimation to 2.4× SW (Fig. 8E). However, differences between salinity groups are largely statistically insignificant and the overall effect is not as pronounced as observed in isolated cell suspensions. Because it was possible with the LSC/ TMA approach to accurately quantify Na$^+$/K$^+$-ATPase abundance per CC we calculated the total Na$^+$/K$^+$-ATPase abundance in all killifish CC by multiplying CC-specific Na$^+$/K$^+$-ATPase fluorescence with the number of CC for each sample (Fig. 9A). The resulting data show a comparable kinetics of increase in Na$^+$/K$^+$-ATPase abundance as for CC hypertrophy: a rapid increase that levels off within 1 week in fish exposed to acute 1× SW transfer and a slow increase that continues steadily for 5 weeks in fish exposed to gradual 2.4× SW transfer. After 5 weeks of acclimation Na$^+$/K$^+$-ATPase abundance is ca. 4.5-fold in 1× SW and 17-fold in 2.4× SW fish compared to FW controls. At that time the relationship between total gill Na$^+$/K$^+$-ATPase and environmental salinity is exponential suggesting that the amount of energy needed to maintain plasma ion homeostasis increases steeply when the salinity exceeds 1× SW (Fig. 9B).

Discussion

Laser scanning cytometry is a useful tool for comparative biology

Laser scanning cytometry (LSC) is a very powerful tool for addressing an increasing variety of biological problems. The technology is less than a decade old and represents a merger between conventional fluorescence microscopy and flow cytometry methods. It is currently being used mainly for biomedical research applications including cell cycle analysis, immunophenotyping and measurement of apoptosis (Bedner et al., 1999; Darzynkiewicz et al., 1999; Claytor et al., 2001). Many LSC applications also represent extremely useful approaches to general problems of comparative experimental biology and LSC technology can be expected to greatly

facilitate the investigation of such problems on a much wider scale. Because LSC analysis is a slide-based technique it allows quantification of cell populations from defined criteria and relocation to/viewing of cells within a population based on those criteria. In this study we have used LSC technology for the first time to reliably and fully automatically quantify CC properties in euryhaline killifish exposed to salinity stress. Using the LSC we were able to consistently detect CC based on DASPMI or Na+/K+-ATPase fluorescence and to exclude cellular debris and cell fragments as well as clusters of multiple CC from the analysis by applying lower and upper size limits. Furthermore, we were able to visually inspect CC during and after scanning to make sure that the detection parameters were optimal. Using the LSC it was possible to scan thousands of CC in each sample within a few minutes resulting in very

accurate counts and size determinations. Thus, the LSC is an ideal tool for CC analysis, offering significant advantages over confocal laser scanning microscopy and conventional flow cytometry approaches that have been used previously (e.g. Van der Heijden et al., 1997; Wong and Chan, 1999).

Kinetics of changes in chloride cell properties

The results of our experiments on dissociated suspensions of CC visualized with the vital stain DASPMI show that the kinetics and extent of CC proliferation are only marginally affected by the salinity acclimation regimen. In contrast, CC hypertrophy depends very strongly on the salinity acclimation regimen. Acute transfer to 1× SW leads to rapid but relatively modest hypertrophy of CC that is complete within 1 week while gradual acclimation to 2.4× SW does not induce
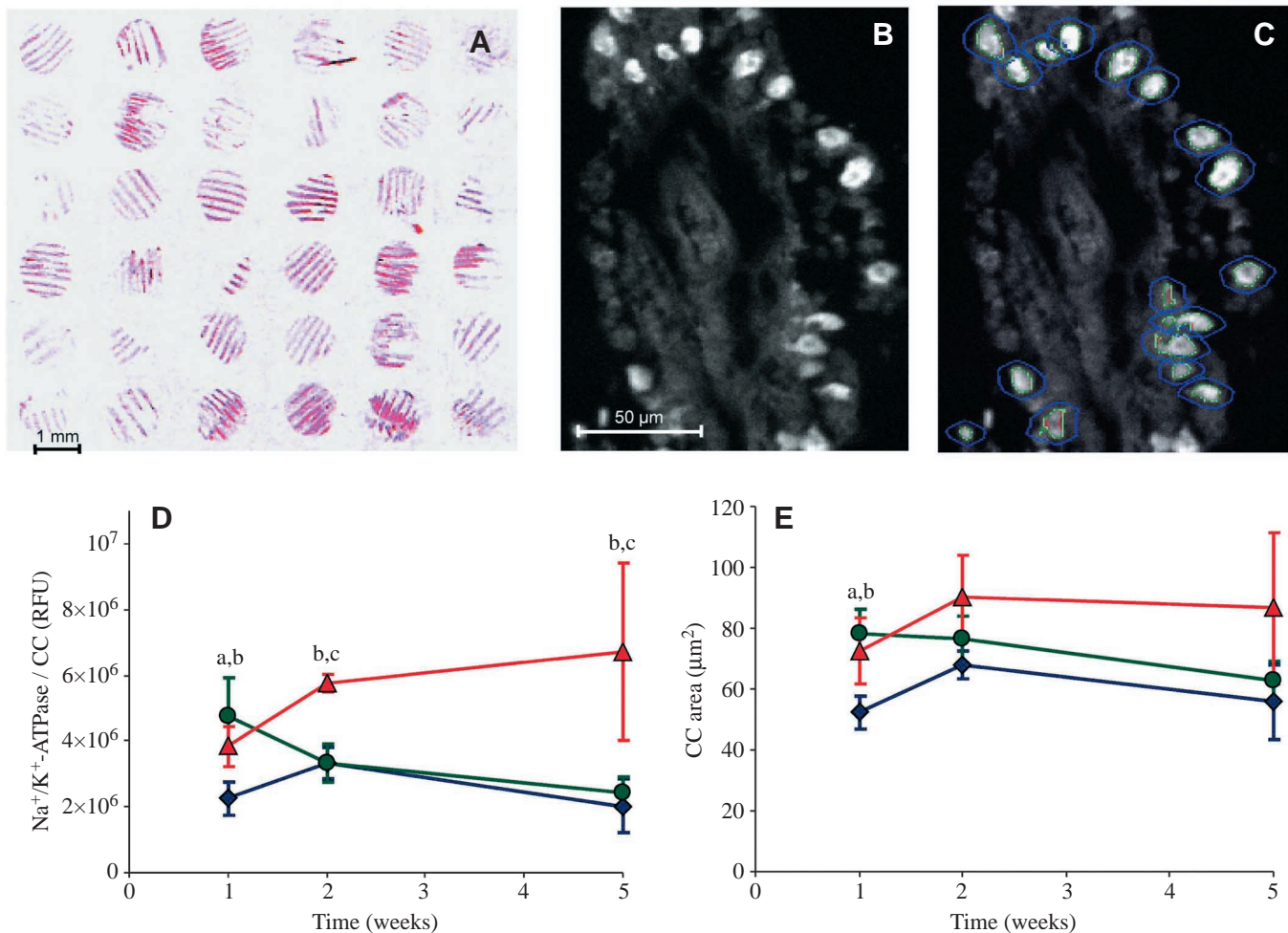

Fig. 8. Quantification of Na+/K+-ATPase per chloride cell (CC) and CC area dependence on salinity and acclimation period. (A) Tissue microarray containing 1 mm cores of gill filament from fish acclimated to FW or SW for different times. Bar, 1 mm. (B) Na+/K+-ATPase antibody combined with PacificBlue-conjugated secondary antibody specifically labels CC. (C) Automatic laser scanning cytometer (LSC) contouring of CC in the same area as shown in A. (D) Quantification of Na+/K+-ATPase content per CC based on LSC analysis (FW, blue diamonds; 1× SW, green circles; 2.4× SW, red triangles). Na+/K+-ATPase in CC is significantly but transiently elevated only at 1 week for fish acclimated to 1× SW ($P<0.05$). In contrast, Na+/K+-ATPase in CC is significantly elevated at all times measured in fish acclimated to 2.4× SW ($P<0.05$) (E) CC area based on contouring of Na+/K+-ATPase fluorescence as shown in B. Although elevated at all times for both 1× and 2.4× SW groups the increase is statistically significant only at 1 week ($P<0.05$; [a]FW vs. 1× SW, [b]FW vs. 2.4× SW, [c]1× SW vs. 2.4× SW). $N=4$ animals for each salinity and time.

significant CC hypertrophy during the first week but leads to a slow and constant increase in CC size over 5 weeks. These differences in salinity-dependent kinetics of CC hypertrophy may be physiologically important. Although it appears that most natural environments are characterized by gradual changes in salinity we know much more about CC responses to acute salinity transfer (e.g. Kültz et al., 1992). Interestingly, CC number in opercular epithelium in *F. heteroclitus* does not change in response to acute transfer from FW to 1× SW (Daborn et al., 2001). These authors suggest that only the area of apical CC exposure varies with salinity in opercular epithelium. Thus, in *F. heteroclitus* salinity-dependent CC proliferation may be regulated differently in gill and opercular epithelia. Such differential regulation of CC proliferation in gill and opercular epithelia contrasts to other euryhaline teleosts, for instance *Oreochromis mossambicus*, where CC number increases in both types of epithelia proportional to external salinity (Kültz et al., 1992). Our data support the notion that CC hypertrophy is much more closely correlated

with salt secretory capacity than CC number (Foskett et al., 1981). Size distribution profiles of CC obtained in this study are very similar to those obtained previously in *O. mossambicus* (Kültz et al., 1992). In FW-adapted fish there is only one population of small mitochondria-rich cells (FW CC) while in SW there are two populations. A minor population is very similar in size to the FW CC and the major population is significantly larger and represents typical SW CC. We hypothesize that the population of small mitochondria-rich cells in SW fish are accessory cells that form multicellular complexes with CC because they display lower DASPMI and Na+/K+-ATPase fluorescence (Katoh et al., 2001). An elegant recent study on *O. mossambicus* larvae indicates that FW CC are transformed into SW CC during salinity acclimation while accessory cells represent a newly differentiated cell type unique to SW fish (Hiroi et al., 1999).

Interestingly, in some euryhaline teleosts such as *Dicentrarchus labrax* the number of CC is lowest in 1× SW and increases upon salinity transfer to FW and 2× SW (Varsamos et al., 2002). In this context, it is important to note that the energy requirements for osmoregulation increase in very dilute environments, and are accompanied by increases in CC number (Laurent and Hebibi, 1989; Perry and Laurent, 1989; Greco et al., 1996; Moron et al., 2003). For our experiments the FW was still relatively rich in major ions (see Materials and methods), and the increased CC numbers in SW relative to FW confirm previous observations under these conditions in other euryhaline teleosts (Foskett et al., 1981; Langdon and Thorpe, 1984; Karnaky, 1986; Kültz et al., 1992).

Tissue microarrays enable quantitative tissue analysis by LSC

In addition to analyzing suspensions of single, dissociated CC we have used LSC to analyze salinity effects on CC and Na+/K+-ATPase in fixed gill tissue. To minimize variability associated with tissue processing, staining and slide scanning and to increase the throughput of samples we constructed tissue microarrays (TMAs) from the filament portion of fixed and paraffin-embedded gills from killifish exposed to FW, 1× SW and 2.4× SW for 1, 2, and 5 weeks. TMA technology was developed only a few years ago and is currently almost exclusively used for clinical pathology (Kononen et al., 1998; Packeisen et al., 2003). It is an extremely useful tool for many areas of histology and immunohistochemical analysis and holds great potential for applications in comparative experimental biology. We decided to combine TMA technology with LSC to assess salinity effects on gill tissue of killifish because the combination of the two provides a very powerful means of quantitative tissue analysis (Gandour-Edwards et al., 2002). This approach worked exceptionally well for quantification of CC-specific Na+/K+-ATPase abundance in dependence of salinity acclimation and it provides a useful tool for quantifying other proteins, DNA and RNA in fish gills in the future.
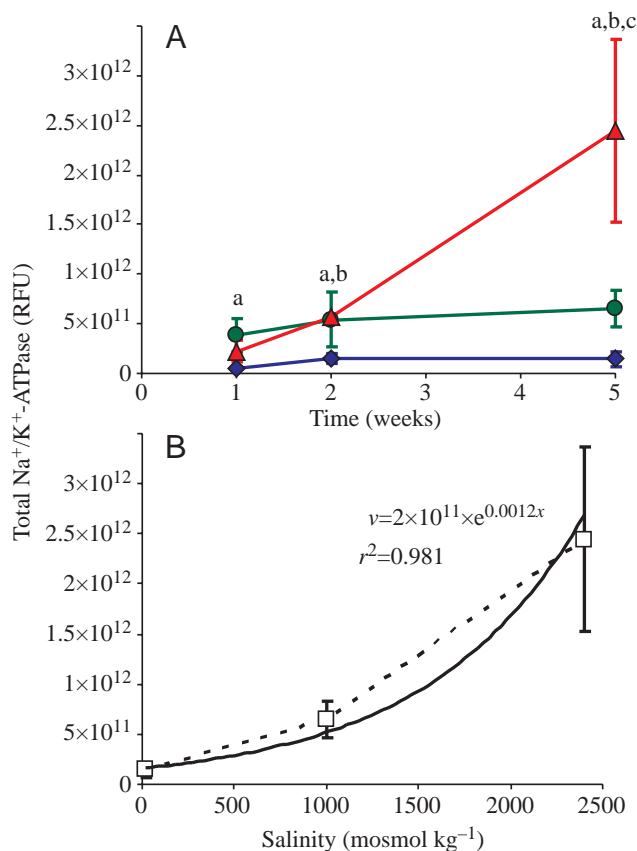

Fig. 9. Total Na+/K+-ATPase content in all gill CC of *F. heteroclitus* acclimated to FW (blue diamonds), 1× SW (green circles), or 2.4× SW (red triangles) expressed as relative fluorescence units (RFU). (A) Time dependence of total Na+/K+-ATPase content at different salinity acclimation regimens ($P<0.05$; [a]FW *vs.* 1× SW, [b]FW *vs.* 2.4× SW, [c]1× SW *vs.* 2.4× SW). (B) Salinity-dependence of total Na+/K+-ATPase content after 5 weeks of acclimation. The data fit an exponential regression with $r^2=0.981$. $N=4$ animals for each salinity and time.

Salinity-dependence of CC and Na+/K+-ATPase in situ

In fixed gill tissue CC can be identified based on their strong

expression of Na$^+$/K$^+$-ATPase (e.g. Van der Heijden et al., 1999). We used this property to automatically segment and quantify CC on tissue microarrays of killifish gills using the LSC. On average 144±29 (mean ± S.E.M.) CC were quantified in each 1 mm diameter piece of gill tissue on the array. This number was too low for accurate quantification of CC because of their heterogeneous distribution. However, this number of CC is sufficient to accurately determine the mean size and Na$^+$/K$^+$-ATPase content of CC in dependence of the different salinity acclimation regimens. Interestingly, CC display much less hypertrophy compared to isolated cell suspensions. This is probably a result of extensive packaging and infoldings of the basolateral membrane, which is particularly pronounced in SW (Karnaky, 1986). Such membrane infoldings are less pronounced after cell dissociation because when isolated and without basement membrane support epithelial cells round up. Therefore, CC size measurements are more accurate when undertaken on suspensions of isolated cells. Despite these limitations for analysis of CC properties the tissue microarray approach proved very useful for quantification of salinity effects on Na$^+$/K$^+$-ATPase content in individual CC and total Na$^+$/K$^+$-ATPase content in killifish gills. In agreement with our finding of different kinetics of CC hypertrophy after acute and gradual transfer from FW to 1× and 2.4× SW we also observed very similar kinetic differences for Na$^+$/K$^+$-ATPase content. The rapid and transient increase in Na$^+$/K$^+$-ATPase content per CC after acute salinity transfer is in agreement with biochemical determinations of Na$^+$/K$^+$-ATPase activity in this species (Mancera and McCormick, 2000). At the new steady state at 5 weeks after salinity transfer there is no difference in Na$^+$/K$^+$-ATPase content per CC between FW and 1× SW groups, consistent with an earlier report (Katoh et al., 2001). However, taking into account the total number of CC, the Na$^+$/K$^+$-ATPase content is ca. 4.5-fold higher in 1× SW compared to FW fish. It should be emphasized that using the approach described here the actual amount of Na$^+$/K$^+$-ATPase is quantified rather than activity of this enzyme, which is reported more frequently than its abundance. The exponential relationship between Na$^+$/K$^+$-ATPase content and environmental salinity suggests that the cost of osmoregulation in euryhaline killifish increases steeply at salinities exceeding regular SW. This is an indirect notion, however, which is based on the assumption that more Na$^+$/K$^+$-ATPase in gills translates into higher expenditure of energy for synthesizing this protein and faster ATP breakdown.

In summary, in this paper we introduce laser scanning cytometry and tissue microarray as powerful tools for comparative experimental biology. Using this approach we have quantified CC properties and Na$^+$/K$^+$-ATPase content in killifish exposed to salinity stress and discovered that these parameters respond with different kinetics to acute and gradual increases in environmental salinity. Such differences in acclimation kinetics could be physiologically very important. They provide a good starting point for further dissection of the regulatory mechanisms underlying salinity adaptation in euryhaline teleosts.

References

Bedner, E., Li, X., Gorczyca, W., Melamed, M. R. and Darzynkiewicz, Z. (1999). Analysis of apoptosis by laser scanning cytometry. *Cytometry* **35**, 181-195.

Bereiter-Hahn, J. (1976). Dimethylaminostyrylmethylpyridiniumiodine (DASPMI) as a fluorescent probe for mitochondria *in situ*. *Biochim. Biophys. Acta* **423**, 1-14.

Bubendorf, L., Nocito, A., Moch, H. and Sauter, G. (2001). Tissue microarray (TMA) technology: miniaturized pathology archives for high-throughput in situ studies. *J. Pathol.* **195**, 72-79.

Buse, P., Tran, S. H., Luther, E., Phu, P. T., Aponte, G. W. and Firestone, G. L. (1999). Cell cycle and hormonal control of nuclear-cytoplasmic localization of the serum- and glucocorticoid-inducible protein kinase, Sgk, in mammary tumor cells: a novel convergence point of anti-proliferative and proliferative cell signaling pathways. *J. Biol. Chem.* **274**, 7253-7263.

Claytor, R. B., Li, J. M., Furman, M. I., Garnette, C. S. C., Rohrer, M. J., Barnard, M. R., Krueger, L. A., Frelinger, A. L. and Michelson, A. D. (2001). Laser scanning cytometry: a novel method for the detection of platelet-endothelial cell adhesion. *Cytometry* **43**, 308-313.

Daborn, K., Cozzi, R. R. F. and Marshall, W. S. (2001). Dynamics of pavement cell-chloride cell interactions during abrupt salinity change in *Fundulus heteroclitus*. *J. Exp. Biol.* **204**, 1889-1899.

Darzynkiewicz, Z., Bedner, E., Li, X., Gorczyca, W. and Melamed, M. R. (1999). Laser-scanning cytometry: a new instrumentation with many applications. *Exp. Cell Res.* **249**, 1-12.

Foskett, J. K., Logsdon, C. D., Turner, T., Machen, T. E. and Bern, H. A. (1981). Differentiation of the chloride extrusion mechanism during seawater adaptation of a teleost fish, the cichlid *Sarotherodon mossambicus*. *J. Exp. Biol.* **93**, 209-224.

Gandour-Edwards, R., Garcia-Williams, A., Folkins, A., Lara, P. N., LaSalle, J. M. and White, R. D. (2002). Laser scanning cytometry detection of HER-2/neu expression in a tissue microarray of bladder urothelial carcinoma. *Modern Pathol.* **15**, 162A.

Greco, A. M., Fenwick, J. C. and Perry, S. F. (1996). The effects of soft-water acclimation on gill structure in the rainbow trout *Oncorhynchus mykiss*. *Cell Tissue Res.* **285**, 75-82.

Hiroi, J., Kaneko, T. and Tanaka, M. (1999). *In vivo* sequential changes in chloride cell morphology in the yolk-sac membrane of Mozambique tilapia (*Oreochromis mossambicus*) embryos and larvae during seawater adaptation. *J. Exp. Biol.* **202**, 3485-3495.

Kamentsky, L. A. (2001). Laser scanning cytometry. *Methods Cell Biol.* **63**, 51-87.

Karnaky, K. J. (1986). Structure and function of the chloride cell of *Fundulus heteroclitus* and other teleosts. *Amer. Zool.* **26**, 209-224.

Katoh, F., Hasegawa, S., Kita, J., Takagi, Y. and Kaneko, T. (2001). Distinct seawater and freshwater types of chloride cells in killifish, *Fundulus heteroclitus*. *Can. J. Zool.* **79**, 822-829.

Kononen, J., Bubendorf, L., Kallioniemi, A., Barlund, M., Schraml, P., Leighton, S., Torhorst, J., Mihatsch, M. J., Sauter, G. and Kallioniemi, O. P. (1998). Tissue microarrays for high-throughput molecular profiling of tumor specimens. *Nat. Med.* **4**, 844-847.

Kültz, D., Bastrop, R., Jürss, K. and Siebers, D. (1992). Mitochondria-rich (MR) cells and the activities of the Na$^+$/K$^+$-ATPase and carbonic anhydrase in the gill and opercular epithelium of *Oreochromis mossambicus* adapted to various salinities. *Comp. Biochem. Physiol.* **102B**, 293-301.

Kültz, D. and Somero, G. N. (1995). Osmotic and thermal effects on *in situ* ATPase activity in permeabilized gill epithelial cells of the fish *Gillichthys mirabilis*. *J. Exp. Biol.* **198**, 1883-1894.

Langdon, J. S. and Thorpe, J. E. (1984). Response of the gill Na$^+$-K$^+$ ATPase activity, succinic dehydrogenase activity and chloride cells to saltwater adaptation in Atlantic salmon, *Salmo salar* L, parr and smolt. *J. Fish Biol.* **24**, 323-331.

Laurent, P. and Hebibi, N. (1989). Gill morphometry and fish osmoregulation. *Can. J. Zool.* **67**, 3055-3063.

Mancera, J. M. and McCormick, S. D. (2000). Rapid activation of gill

Na$^+$,K$^+$-ATPase in the euryhaline teleost *Fundulus heteroclitus*. *J. Exp. Zool.* **287**, 263-274.

Mocellin, S., Fetsch, T., Abati, T., Phan, G. Q., Wang, J., Provenzano, M., Stroncek, D., Rosenberg, S. A. and Marincola, F. M. (2001). Laser scanning cytometry evaluation of MART-1, gp100, and HLA-A2 expression in melanoma metastases. *J. Immunother.* **24**, 447-458.

Moron, S. E., Oba, E. T., De Andrade, C. A. and Fernandes, M. N. (2003). Chloride cell responses to ion challenge in two tropical freshwater fish, the erythrinids *Hoplias malabaricus* and *Hoplerythrinus unitaeniatus*. *J. Exp. Zool.* **298A**, 93-104.

Pachmann, K., Zhao, S. R., Schenk, T., Kantarjian, H., El Naggar, A. K., Siciliano, M. J., Guo, J. Q., Arlinghaus, R. B. and Andreeff, M. (2001). Expression of bcr-abl mRNA in individual chronic myelogenous leukaemia cells as determined by *in situ* amplification. *Br. J. Haematol.* **112**, 749-759.

Packeisen, J., Korsching, E., Herbst, H., Boecker, W. and Buerger, H. (2003). Demystified... Tissue microarray technology. *J. Clin. Pathol.* **56**, 198-204.

Perry, S. F. and Laurent, P. (1989). Adaptational responses of rainbow trout to lowered external NaCl concentration: contribution of the branchial chloride cell. *J. Exp. Biol.* **147**, 147-168.

Van der Heijden, A. J. H., van der Meij, J. C. A., Flik, G. and Bonga, S. E. W. (1999). Ultrastructure and distribution dynamics of chloride cells in tilapia larvae in fresh water and sea water. *Cell Tissue Res.* **297**, 119-130.

Van der Heijden, A. J. H., Verbost, P. M., Eygensteyn, J., Li, J., Bonga, S. E. W. and Flik, G. (1997). Mitochondria-rich cells in gills of tilapia (*Oreochromis mossambicus*) adapted to fresh water or sea water: quantification by confocal laser scanning microscopy. *J. Exp. Biol.* **200**, 55-64.

Varsamos, S., Diaz, J. P., Charmantier, G., Flik, G., Blasco, C. and Comes, R. (2002). Branchial chloride cells in sea bass (*Dicentrarchus labrax*) adapted to fresh water, seawater, and doubly-concentrated seawater. *J. Exp. Zool.* **293**, 12-26.

Wong, C. K. C. and Chan, D. K. O. (1999). Chloride cell subtypes in the gill epithelium of Japanese eel *Anguilla japonica*. *Am. J. Physiol* **277**, R517-R522.